Journal of Solar Energy Research (JSER)

Journal homepage: www.jser.ut.ac.ir

Experimental Assessment of A Solar-Powered Lithium Bromide-Water Absorption Cooling System for Sustainable Air Conditioning in Hot Climate Regions

Sanaa M. Hadi[a], Mushtaq I. Hasan[a], Mudhar A. Al-Obaidi[b*], Farhan Lafta Rashid[c], Moneer H. Tolephih[d]

[a]*Mechanical Engineering Department, College of Engineering, University of Thi-Qar, Iraq*
[b]*Technical Instructor Training Institute, Middle Technical University, Baghdad 10074, Iraq*
[c]*Petroleum Engineering Department, College of Engineering, University of Kerbala, Karbala 56001, Iraq*
[d]*College of Engineering, Al-Naji University, Baghdad, Iraq*

ARTICLE INFO

Article Type:

Research Article

Received:2025.12.28
Accepted in revised form:2026.07.01

Keywords:
Solar collectors; Heat pipe; Absorption system; Solar energy; Water- Lithium bromide solution; Experimental absorption cooling system

A B S T R A C T

This research conducted an experimental study by looking at a solar-powered single-effect absorption cooling system with 1 kW power under hot climate conditions in Nasiriyah, Iraq. The working fluid is a 55% solution of lithium bromide-water and the thermal energy is supplied by an evacuated tube solar collector. The developed system is assessed by measuring the correlation between solar radiation, ambient temperature, and component temperature tested in August 2024 while the solar radiation is at its peak intensity of 945 W/m^2. The outcomes indicate that an increase in solar radiation can result in an increase in the temperature of the generator that boosts the evaporation of refrigerant and the overall performance of the system. The best operational efficiency can be attained when the generator operates at 94 ^oC and evaporator at 28 ^oC. The results verify that solar-driven absorption cooling is a technical and a sustainable alternative to traditional cooling systems in highly solar-irradiated regions, which has great potential of cutting down on the reliance on fossil fuels and limiting environmental impact.

*Corresponding Author Email: dr.mudhar.alaubedy@mtu.edu.iq

Cite this article: Hadi, S. M. , Hasan, M. I. , Al-Obaidi, M. A. , Rashid, F. Lafta and Tolephih, M. H. (2026). Experimental Assessment of A Solar-Powered Lithium Bromide-Water Absorption Cooling System for Sustainable Air Conditioning in Hot Climate Regions. Journal of Solar Energy Research, 11(3), 3924-3926. doi: 10.22059/jser.2026.409023.1698

DOI: 10.22059/jser.2026.409023.1698

1. Introduction

The air conditioning in hot countries is becoming one of the most significant forms of energy consumption due to the growing of building loads and the corresponding growth in user demand for thermal comfort. As a result, during the warmest summer days, the electrical power consumption of refrigeration equipment starts to produce load in the supply network [1]. Indeed, the combination of solar energy into air conditioning systems would strongly align with sustainability aims as it aids to reduce the dependence on fossil fuels besides reducung the greenhouse gas emissions [2,3]. Therefore, the adaption of solar-powered solutions would deliver a dual advantage, improving energy efficacy in addition to promoting ecological integrity. This is in a comparison to traditional air conditioning systems that require a considerable specific energy consumption. In other words, the global transition towards renewable energy sources can be attained via harnessing solar energy, which would enable to resolve the urgent request for sustainable cooling solutions in hot climate regions [4].

The majority of buildings use vapor compression chillers that are powered by electricity. By 2050, it is currently predicted that the energy used for air conditioning would have increased tenfold [5]. However, a number of halogenated organic refrigerants, including hydro chlorofluorocarbons (HCFCs) are still used in mechanical compression chillers and have been outlawed or are in the process of being outlawed as they continue to contribute to the ozone layer's thinning. Solar-driven cooling systems appear to be a good substitute for traditional electrical-driven compression units in terms of improving the building's energy efficiency as they accomplish reduced greenhouse gas emissions and main energy savings for solar percentages over about 50% [6].

Referring to the use of lithium bromide (LiBr)/water (H_2O) as an absorption cooling system, there are a number of published studies that encountered with several simulation investigations. First of all, Bani Younes et al. [7] provided a simulation of a 10 kW LiBr–H_2O absorption chiller for a 100 m^2 tiny area divided into three distinct zones in Australia. Barghouti et al. [8] conducted research on the sun absorption cooling system's viability and sensitivity in Tunisia. The researchers concluded that the cooling demand for a 150 m^2 house requires a 0.8 m^3 storage tank, 30 m^2 of flat plate solar collectors, and an 11 kW absorption chiller. Ketjoy et al. [9] examined how well a 35 kW LiBr– H_2O absorption chiller performed when combined to 72 m^2 of evacuated tube collectors (ETC) and an auxiliary boiler. The findings indicated that the solar absorption system functioned efficiently, with 2.63 m^2 of collector area per kW of air conditioning. Martínez et al. [10] demonstrated a comparison between a solar cooling system simulation created using TRNSYS software and actual data from a system in Alicante, Spain. The air-cooling system included a 1 m^3 hot storage tank and a 17.6 kW LiBr–H_2O absorption chiller. The real data indicated that the absorption chiller's coefficient of performance (COP) was 0.691, while the simulated system achieved a COP of 0.73. The findings also demonstrated a close similarity between the simulated and measured data. Burckhart [11] outlined a 4000 m^2 building that includes offices, labs, and a public space. A 95 kW LiBr–H_2O absorption chiller was powered by hot water that was heated to about 90 °C by a 250 m^2 array of vacuum tube solar thermal collectors. Martínez et al. [12] conducted numerical and experimental investigations, where the COP values were indicated to be 0.73 and 0.691, respectively, with a variation of 5.48%. At Cardiff University in the United Kingdom, an experimental testing was carried out by Peuser et al. [13] on a 4.5 kW solar-powered LiBr–H_2O absorption cooling system using a 12 m ETC. The average COP achieved during the testing was 0.63, with the generator temperature reaching 80 °C. The average peak global sun radiation recorded during the testing was 812 W/m^2. A theoretical and experimental investigation of the LiBr–H_2O single-effect absorption chiller was also conducted by Balghouthi et al. [14]. It had a 55 kW cooling capacity and was powered by ETC. The findings showed that a COP value of 0.69 was attained, the cooled water was obtained at a temperature of 7 °C, and the maximum generator did not exceed 100 °C.

Hashemian and Noorpoor [15] proposed an innovative multi-generation plant that uses solar and wind energy. Another idea of a hybrid system that generates power by integrating wind and a steam Rankine cycle was suggested by the researchers. The system aims at generating hydrogen by using a proton exchange membrane electrolyzer and ammonia by a reactor. The novel system did not only produce electricity but is a complete power (44.8 MW) and heating (20.64 MW), cooling (123.9 MW), hydrogen (263.1 kg/h) and ammonia (106.48 kg/h) generating system. A thermo-economic-environmental investigation indicated positive performance with high energetic (83.65%) and exergetic (17.97%) factor and exergo-environmental impact factor (0.91) and a total product cost rate of 1.44$/s. In new design, Hashemian and Noorpoor [16] presented a multi-generation system design, which is founded on the use of biomass and solar energy to produce electric power, heating, cooling, hydrogen, and potable water. The system was made up of a steam Rankine cycle, two effect absorption chiller, proton exchange membrane electrolyzer, multi effect desalination and parabolic trough solar collector. This showed that the multi-generation system can achieve energy efficiency, exergy efficiency, improve the total product cost rate and exergo-environmental impact of 82.4%, 14%, 0.84 $/s and 0.15, respectively. Lastly, the application of multi-criteria optimisation method that is grounded on a genetic algorithm was used to define the ideal design of the system based on enhancement of the thermodynamic and thermos-economic performance.

In the past, extreme climatic conditions of Iraq have been referred to in some simulation studies, but none have actually built and tested a solar absorption cooling system under the actual operating conditions of Nasiriyah, where ambient temperature can reach as high as 50 °C and the intensity of solar radiation can reach 945 W/m². In addition to providing these unprecedented experimental performance data, which have never been reported in the literature, our study presents a replicable, cost-effective fabrication of a 1 kW LiBr-H_2O single-effect absorption cooling system using locally available components, thus offering a practical and accessible blueprint for the implementation of sustainable cooling technologies in other hot climate regions with similar energy challenges. This experimental validation brings the discussion from theoretical evaluation to real proof and results into the fact that solar driven absorption cooling is technically feasible and economically viable in extreme climatic conditions. Through this important research gap, both empirical findings and a hands-on design approach are presented that could be readily applied by researchers and practitioners in high-solar-irradiance regions facing increasing cooling loads and drives the transition towards sustainable air conditioning solutions worldwide.

2. Description of cooling system

2.1 Absorption cycle

A single-effect solar-driven absorption cooling system consists of an absorption chiller, a solar thermal collector, and additional components including pumps, valves, and thermal storage. The basic configuration of the chiller (Figure 1) includes four main components: the evaporator, absorber, generator, and condenser. Solar thermal energy input (state 17) to the generator facilitates refrigerant (water) evaporation from the LiBr-water solution, resulting in a concentrated solution. The vaporized refrigerant subsequently undergoes condensation in the condenser (stage 7). Simultaneously, the regenerated absorbent solution, via a solution heat exchanger (SHX) process (stages 4–5), returns to the absorber. Expansion valves induce pressure and temperature drop in both the refrigerant and solution streams. In the evaporator, the refrigerant absorbs heat from the cooling load, evaporating and exiting as saturated vapor (stage 10). This vapor is then absorbed by the concentrated solution within the absorber. Ambient air typically facilitates heat rejection from the condenser and absorber. Refrigerant vapor from the evaporator is absorbed by the concentrated solution in the absorber, generating a dilute solution. Heat rejection from the condenser and absorber is typically accomplished via ambient air cooling (states 11–12, 15–16) or, alternatively, using a cooling tower (not shown). The cycle is completed by pumping the dilute solution from the absorber back to the generator (states 1–3) at a high pressure.

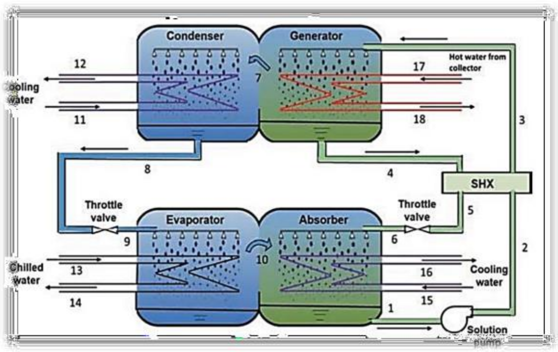

Figure 1. Single effect LiBr-H_2O absorption chiller [14]

2.2 Solar collector

Evacuated tube collectors with heat pipes are solar thermal devices used to capture and transfer solar energy. They are particularly effective at converting sunlight into heat with high efficiency. The solar collector, a key part of the absorption refrigeration cycle, converts solar energy into heat energy by heating water, which then drives an absorption chiller. Liquid water is used for heat transfer due to its high heat capacity and thermal conductivity. The components of evacuated tube heat pipe are shown in Figure 2.

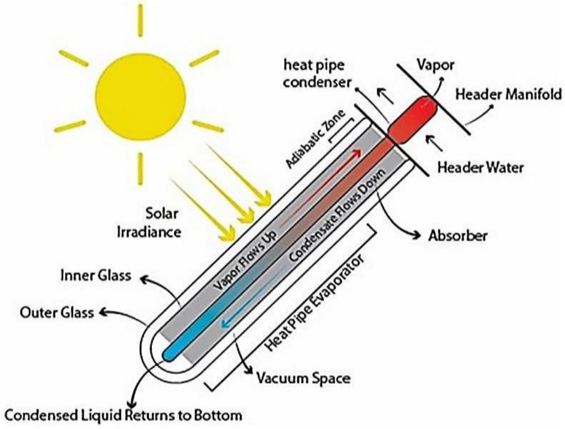

Figure 2. A schematic diagram of the heat pipe evacuated tube collector

A solar collector consists of several evacuated glass tubes. These tubes are designed to minimise heat loss by creating a vacuum between the inner and outer layers of the tube. This vacuum acts as an insulating layer, greatly reducing heat transfer by conduction and convection. There is an absorber plate inside each tube, which is coated with a selective material (usually black) that efficiently absorbs solar radiation. When sunlight hits the absorber plate, it converts solar energy into heat. Inside the glass tube is a heat pipe, a sealed tube containing a small amount of working fluid (usually water or a refrigerant). The heat pipe is connected to the absorber plate and has a two-phase heat transfer mechanism.

- Evaporation: As the temperature of the absorber plate increases due to solar radiation, the working fluid inside the heat pipe evaporates and turns into vapor.

- Heat transfer: The vapor rises to the top of the heat pipe, carrying the absorbed heat with it. At the top of the heat pipe is a cold section or heat exchanger (which can be in contact with a heat transfer fluid or a storage tank). Here, the steam releases its heat and condenses back into a liquid. The liquid then returns to the bottom of the heat pipe (due to gravity or capillary action) to be heated again, and the cycle repeats.

The solar collector thermal efficiency is expressed in Eq. 1, which considers the linear and quadratic terms of the temperature difference [4,5].

$$\eta_c = \eta_0 - a_1 \frac{\Delta T}{I_T} - a_2 \frac{(\Delta T)^2}{I_T} \qquad (1)$$

ΔT: The temperature difference between the ambient temperature (T_a) and the collector outlet temperature (°C).

I_T: Total incident solar radiation on the collector (W/m²)

η_c: The optical efficiency.

η_0 = The efficiency when there is no temperature difference, which is deemed as zero-loss efficiency.

a_1 and a_2: First and second slope coefficients, respectively.

3. Experimental rig fabrication

In this research, a (1 KW) solar-powered absorption cooling system was designed, consisting of an evaporator, condenser, absorber, generator and a heat exchanger. The appropriate dimensions for all parts were determined, and the manufacturing step was made according to the following steps:

1. The shell and coil type evaporator, absorber, condenser, generator was designed.

2. The shell was made of (2 mm) galvanized iron, cut and bent to the required shape, and the parts were welded using an electric welding machine (Figure 3). The coil was made of 5/8” copper pipes according to the number of turns calculated for each part (Figure 4), and these coils were fixed inside the shell for each part using copper welding (Figure 5).

3. The heat exchanger is designed as a double tube type, where a (1/2” inch) copper tube was selected and installed inside another (1 inch) copper tube, (1.5 m) long, and welded between the generator and the absorber.

4. Water pumps were installed for each of (generator, condenser, evaporator, and absorber).

5. A capillary tube was placed between the condenser and the evaporator (it is a copper tube 2.5

meters long and 1.5 mm in diameter) as depicted in Figure 6.

6. Using a radiator and fan as a cooling tower and installed on top of the condenser.

7. Formation of the iron structure with dimensions (1 m, 1 m, 2 m) and connecting all parts of the absorption cycle together using copper pipes with welding.

8. All parts of the cycle are insulated with thermal insulation. Figure 7 shows the final shape of the absorption cooling system.

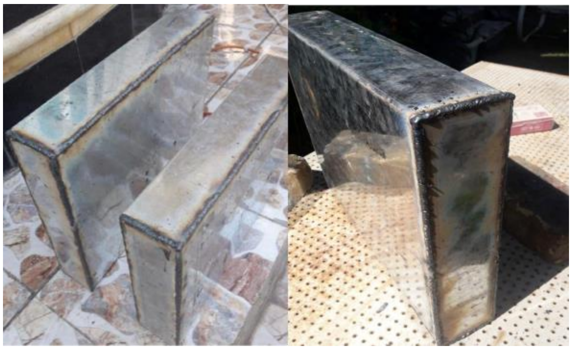

Figure 3. The synthesized shells

Figure 4. Mechanism of the coil manufacturing for the part

Figure 5. Mechanism of manufacturing the coil inside the shell for the parts

Figure 6. Capillary tube

Figure 7. Absorption system cycle

4. Experimental procedures

The tests of the current research were conducted on the solar-powered absorption cooling system in Dhi Qar- Iraq during August of 2024. The absorption cooling system includes the following parts (generator, condenser, evaporator, absorber, heat exchanger). These were evacuated and injected with a solution ($LiBr$-H_2O) at a concentration of 55% into the generator, then connected the pumps to the electrical control system to start the system. The solar-powered absorption cooling system continuously operated from (8 am to 5 pm), and readings were taken every hour. The readings included the entry and exit temperatures for each part of the system for the shell and the coil. The entry and exit temperatures of the solar collector were also taken every hour. It was noted that after the generator temperature reaches 80 °C, evaporation occurs in the solution to start the actual operation of the system, which is usually at (10–11 am). The temperature readings were recorded through the thermo-couples connected to the recorder device for temperature (data logger). The pressure readings were also recorded by having pressure gauges, one between the generator and the condenser and the other between the condenser and the evaporator. Furthermore, the amount of refrigerant flow was measured by having a flow-meter between the condenser and the evaporator. Figure 8 demonstrates a flowchart of the research methodology.

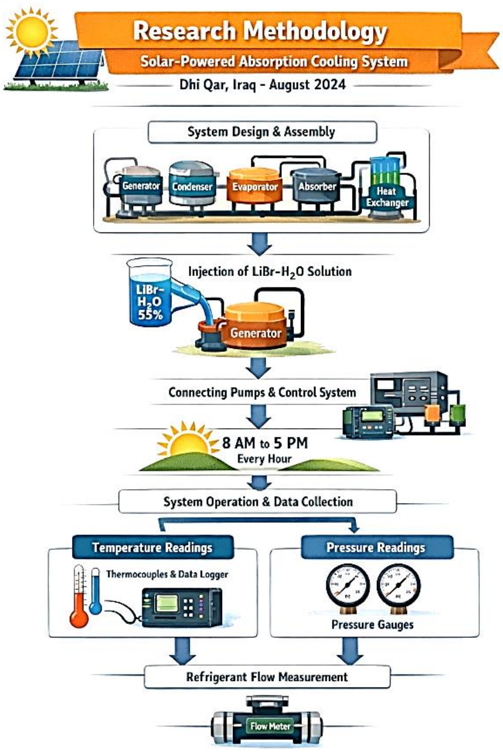

Figure 8. Flowchart of the research methodology

5. Weather Data

The determination of the performance of solar-powered cooling systems requires accurate data of the solar radiation. In this research, the total solar radiation that reached a horizontal surface in Nasiriyah city, Dhi Qar-Iraq (longitude 46.22ºE, latitude 31.13ºN) were measured and sampled throughout the period of the experiment (June to September 2024). Meteorological data such as ambient temperature and relative humidity together with dust conditions and cloud cover was availed by the Nasiriyah Meteorological Station during the period of the testing. These readings were particularly taken with the aim of establishing the amount of heat energy that can be used to drive the 1 kW absorption cooling system through the evacuated tube collector array.

The intensity of solar radiations was measured continuously as the system was operating in the time period of 8:00 AM to 5:00 PM per day. The values of solar radiations were found to be 0 W/m^2 in the morning and evening times and hit its peak of 945 W/m^2 in the daytime. This maximum radiation level can be measured on several days in August 2024, and this is actually the solar power of the test location, which had a direct effect on the thermal power input to the generator. The diurnal change of the intensity of the solar radiation on the 5th of August 2024, with a slow rise in the morning hours, reaching its peak between 12.00 PM and 1.00 PM and then a gradual decrease during the afternoon. The combination of these measured radiation values with the respective ambient temperature values gave the basic input parameters in assessing the performance of the absorption cooling system under the realistic Iraqi weather conditions. In contrast to the general theoretical descriptions of solar radiation, the meteorological data provided in the paper would be the real-life conditions under which the system is to be tested, so that the analysis of the system performance would be more relevant to the operations in the hot climatic areas.

6. Results and discussion

Figure 9 shows the variation of air temperature against operational hours of the day for the city of Nasiriyah City-Iraq at longitude (46.22) and latitude (31.13) on 5th August 2024. Figure 9 shows that there is a gradual increase in temperature in a response to an increase in solar radiation, reaching its highest value of 50 °C at around 1:00 PM. This maximum temperature in such time can be attributed to the intense solar radiation falling vertically.

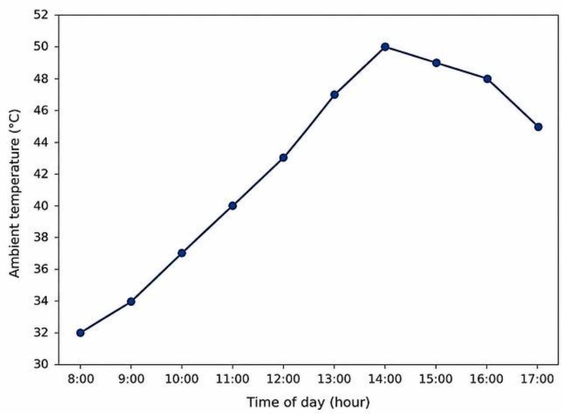

Figure 9. Measured ambient temperature (℃) at 5th August 2024

Figure 10 shows the relationship between the temperature of the generator and operational time for

5th of August 2024. Figure 10 depicts an increase in generator temperature with the operating time, which can be ascribed to an increase in the hot water temperature coming from the solar collector as a consequence to an increase in the ambient temperature and an increase in the intensity of solar radiation falling on the collector. The generator is designed to convert solar thermal energy into solvent vapor. As the system continues to operate, more heat is absorbed and transferred to the generator, increasing its temperature. As operation continues, the generator can be in a more efficient state, causing the temperature of the generator to rise as the thermal process improves. In certain systems, the chemical activity within the generator may increase over time, causing the temperature to rise. As more heat is generated within the generator, more heat is transferred to the absorbing fluid, contributing to the overall temperature of the generator. Generator overheating is a normal part of the cooling cycle and can affect the efficiency of the system, and thus proper temperature management is required to avoid potential damage or loss of efficiency due to excessive temperatures. In other words, it can be said that the system should be designed well so that temperatures are properly controlled to ensure efficient and safe operation. The highest temperature of the generator was 94 °C at 3 pm and then it started to decrease due to the decrease in the ambient temperature as well as the solar radiation.

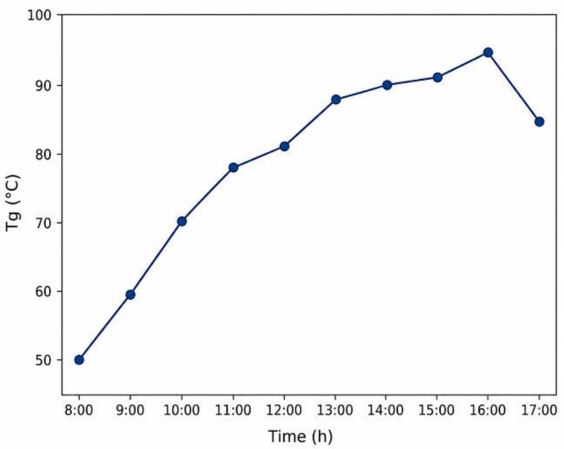

Figure 10. Variation of generator's temperature against operational time (hour)

Figure 11 shows the difference between the number of daily operating hours and the condenser temperature. Figure 11 shows that at the start of operation and before the system reaches equilibrium, the condenser temperature is close to the ambient temperature. When the system starts operating, the solar collector heats the solution, which increases the temperature of the condenser. At this point, the vapor pressure rises and condenses at the condenser, where it is cooled by (water coming from the cooling tower inside a coil). During continuous operating hours, the condenser begins to lose more heat, as the fluid vapor is converted into a liquid, better cooling can occur by the water coming from the cooling tower. Furthermore, with increasing operating hours, the condenser temperature eventually reaches a dynamic equilibrium, meaning that the rate of heat loss and system performance become more efficient and reach a stable state, where the condensers can operate more efficiently for a longer period. As the cooling process continues, the condenser temperature decreases. The decrease in temperature contributes to the reversal of the cooling cycle more efficiently, which helps to improve the absorption and cooling process in general. In other words, the process of decreasing the condenser temperature with increasing operating hours can be considered as a sign of the efficiency of the system in performing the cooling process, as it becomes more effective in converting solar energy into cooling energy.

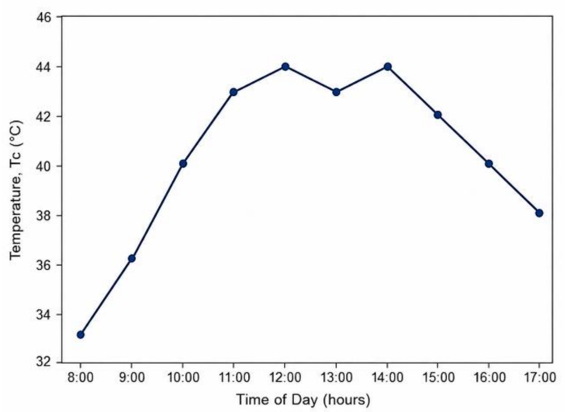

Figure 11. Variation of condenser's temperature against operational time (hour)

Figure 12 shows the evaporator temperature against the operational time of the absorption cooling system. When the absorption cooling system starts up, the evaporator experiences an increase in temperature as the system was in an imbalance state and the heat absorption process inside the evaporator may not have started effectively yet. Also, there may not be enough flow from the refrigerant to the evaporator, which would lead to a rise in temperature even under the influence of the heat available from the surrounding environment. As time passes, the evaporator temperature begins to decrease because the refrigerant begins to absorb the heat in the evaporator more efficiently and the evaporator temperature gradually decreases. Also, the liquid refrigerant moves to the evaporator more regularly, which improves the cooling process. After passing several hours of operation, the system operates in a balanced manner, which contributes to the continuous extraction of heat from the surrounding environment, and thus the temperature in the evaporator decreases. It can be said that the behavior of the evaporator temperature in the solar-powered absorption refrigeration cycle is characterized by an initial transient increase followed by a gradual decrease that reflects the stability and efficiency of the system during the cooling process.

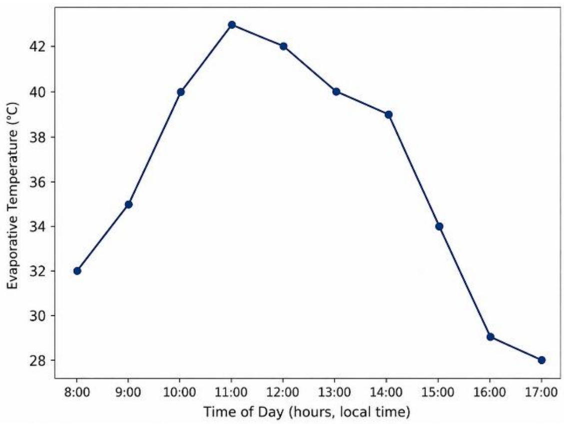

Figure 12. Variation of evaporator temperature against operational time (hour)

Figure 13 shows the relationship between the absorber temperature and progress of operational time for the absorption refrigeration cycle. Figure 13 indicates that when the system starts up, the absorber temperature rises due to the high temperature of the generator, where the solution is separated in the generator, and thus the temperature of the salt (LiBr) coming from the generator to the absorber rises. Also, the cold liquid may not be absorbed effectively, which leads to heat accumulation in the absorber. With continuous operation and the absorber being supplied with heat from the generator or solar collector, the system begins to operate more efficiently. The refrigerant begins to move from the evaporator to the absorber better, which leads to a reduction in the absorber temperature. Over time, the absorption process between the refrigerant (water) and the absorber (lithium bromide) is more effective. When the refrigerant is absorbed into the absorber, some heat is released, which leads to a reduction in the absorber temperature. After a period of operation, a more stable thermal equilibrium is reached, as the absorber improves the process of absorbing heat from the refrigerant, and the required performance of the system is achieved at lower temperatures. As the refrigerant heating phase is completed and an efficient absorption process is achieved, the absorber temperature decreases, increasing the efficiency of the cycle and making the system more effective in providing cooling. Also, as the refrigeration system approaches the equilibrium point, energy efficiency improves and the system continues to operate satisfactorily under varying thermal loads.

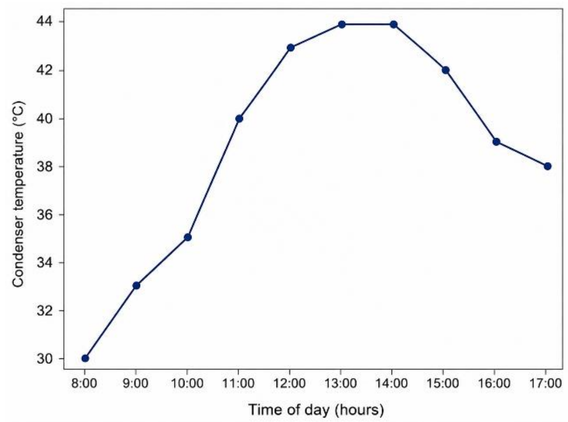

Figure. 13. Variation of condenser temperature against operational time (hour)

Figure 14 shows the relationship between the Refrigerant vapor (water) coming out of the generator against the operational time. Figure 14 elucidates that at the beginning of operation, all components of the system, including the generator, are at ambient temperature and the LiBr-water solution in the generator is relatively cool. When the solar collector begins supplying heat, a significant heat flux is initially applied to the generator. The generator's thermal mass (the heat capacity of the generator and its contents) is relatively low compared to the heat input rate. Because of the high heat flux and low thermal mass, the temperature of the LiBr-water solution in the generator rises rapidly. This rapid temperature increase is further amplified by the fact that the solution is initially far from its boiling point. Initially, the vapor pressure of the water in the solution is low, so the rate of vaporization is relatively slow. This means that much of the heat input goes into raising the temperature of the solution rather than into vaporization. As the system continues to operate and the temperature of the solution increases, the vapor pressure of the water rises significantly. This leads to a higher rate of water vaporization; larger portion of the heat input now goes into vaporizing the water rather than simply raising the temperature of the solution. This causes the rate of temperature increase to slow down. The system gradually approaches a steady-state condition where the rate of heat input from the solar collector is balanced by the rate of heat removal through vaporization and heat losses to the surroundings. At this point, the temperature of the refrigerant vapor stabilizes.

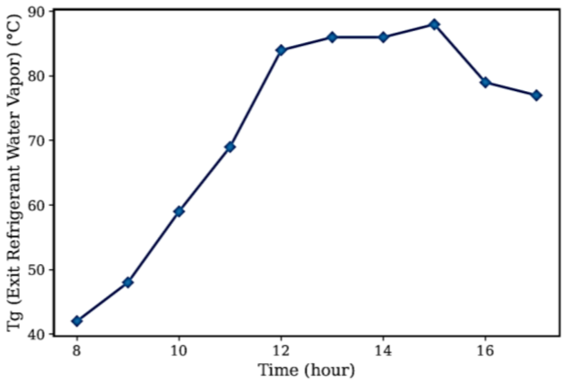

Figure 14. Variation of exit refrigerant water vapor temperature against operational time (hour)

The temperature profile of LiBr solution coming out of generator is shown in Figure 15. The evaporation of the refrigerant (water) from the LiBr-water solution is an endothermic process. Thus, it requires heat energy and this heat energy is drawn from the surrounding solution, causing a clear decrease of its temperature. The more water (refrigerant) evaporates from the solution, the lower the temperature of the remaining solution (concentrated solution) slightly, but the average temperature of the generator as a whole may still be high due to the continued flow of heat from the solar energy source.

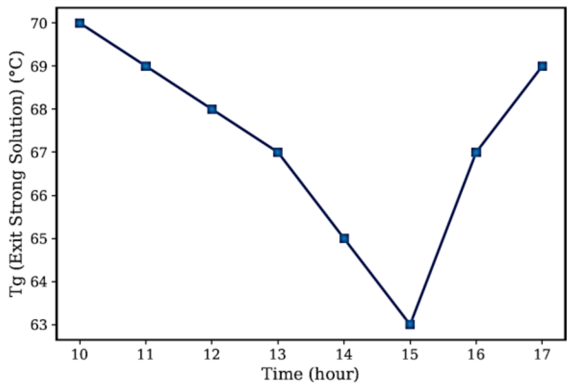

Figure 15. Variation of exit strong solution temperature against operational time (hour)

Figure 16 depicts the relationship between the temperature of the Refrigerant vapor (H_2O) coming out of the generator and the operational time. At the beginning of operation, all components of the system, including the generator, are at ambient temperature and the LiBr- H_2O solution in the generator is relatively cool. When the solar collector begins supplying heat, a significant heat flux is initially applied to the generator. The heat capacity of the generator is relatively low compared to the heat input rate. Because of the high heat flux and low thermal mass, the temperature of the LiBr-H_2O solution in the generator rises rapidly. This rapid temperature increase is further amplified by the fact that the solution is initially far from its boiling point. Initially, the vapor pressure of the water in the solution is low, and therefore the rate of vaporization is relatively slow. This means that much of the heat input goes into raising the temperature of the solution rather than into vaporization. As the system continues to operate and the temperature of the solution increases, the vapor pressure of the water rises significantly. This leads to a higher rate of water vaporization, larger portion of the heat input now goes into vaporizing the water rather than simply raising the temperature of the solution. This causes the rate of temperature increase to slow down. The system gradually approaches a steady-state condition where the rate of heat input from the solar collector is balanced by the rate of heat removal through vaporization and heat losses to the surroundings. Specifically, the temperature of the refrigerant vapor stabilizes at this point.

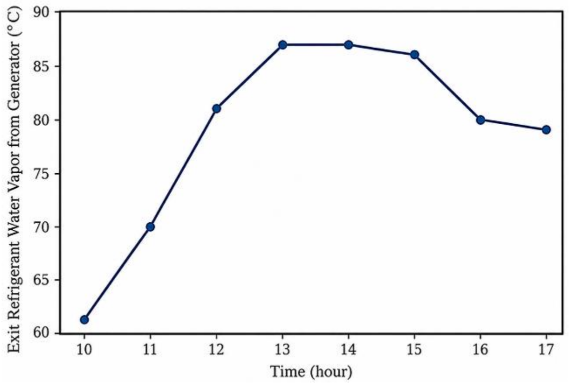

Figure 16. Variation of exit refrigerant water vapor temperature from generator against operational time (hour)

Figure 17 depicts the relationship between the efficiency of evacuated tube solar collector and the required collector area. It can be stated that as the incident solar radiation increases, the required area of the evacuated tube solar collector can be decreased. This is because the amount of solar energy available for absorption increases, which means that the same amount of heat can be obtained using a smaller collector area. Therefore, as the solar radiation increases, it becomes possible to reduce the size of the solar collector to maintain the same levels of efficiency or the required thermal energy production. However, other factors such as the design of the collector and the efficiency of the systems associated with it, as well as changes in climatic conditions and the intensity of solar radiation.

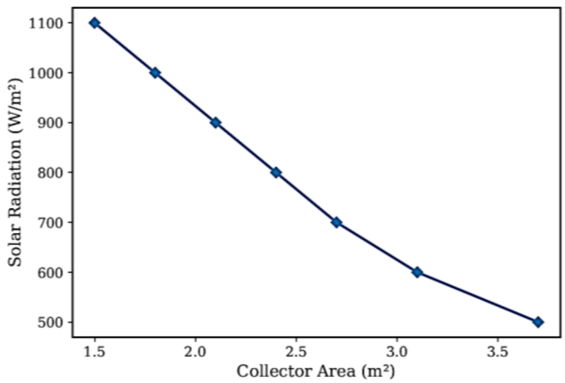

Figure 17. Variation of solar radiation (W/m^2) against the area of collector (m^2)

Figure 18 shows the relationship between the efficiency of a solar collector and the area required for a thermally evacuated tube solar collector. Figure 18 ascertains that when the efficiency of a thermally evacuated tube solar collector increases, the area required to generate the same amount of energy decreases because a more efficient solar collector converts more solar radiation into heat. This means that it can collect a greater amount of solar energy from the same area. Therefore, if the efficiency increases, the system will require less area to generate a given amount of thermal energy. Evacuated tubes also provide better insulation, which reduces heat loss to the surrounding environment. When heat loss decreases, it becomes possible to use a smaller size of tubes to achieve the same efficiency, which reduces the need for a larger area.

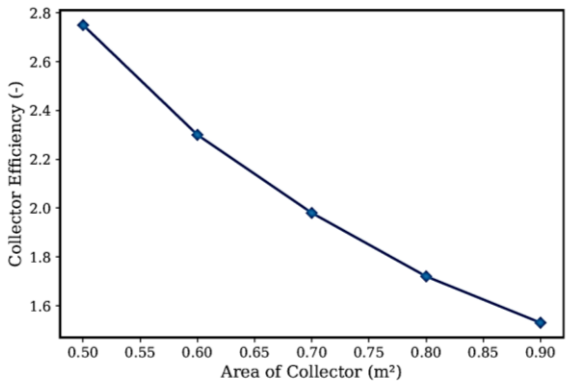

Figure 18. Variation of collector efficiency against the area of collector (m^2)

7. Economic and Environmental Implications

Economically, the 1 kW solar-powered absorption cooling system proposed would have great cost advantages in the long term even though it would demand more initial capital than traditional vapor compression units. The system makes use of free solar thermal which in turn consumes a lot of electricity in terms of air conditioning during the peak season when the electricity rate at such time is the highest. Specifically, in a typical residential case in Nasiriyah, where the sun is very bright, 8-10 hours per day, the system would be used to offset about 80-90% of the electricity bill in cooling, which would create a simple payback period of about 4-6 years under the current Iraqi electricity rates and estimated fossil fuel savings. The system has several sustainability benefits, environmentally: it uses an ozone-safe LiBr-H_2O working pair with no ozone depletion potential, it does not produce direct greenhouse gas emissions as synthetic refrigerants do and it has decreased indirect CO_2 emissions because it replaces electricity production based on fossil fuels. With an average solar radiation of 800 W/m2 and 300 sunny days per year, the system will be able to avoid 1.5-2.0 tons of

CO_2 emissions each year in relation to an electrically-powered chiller of the same capacity. These results indicate that solar absorption cooling is not only a technically feasible solution to hot climate areas but it is also economically viable and environmentally friendly that meets the decarbonization target of the world and the increasing demands of Iraq towards sustainable cooling technologies.

8. Conclusions

The current research experimentally investigated the feasibility of fabricated 1 kW solar-powered single-effect absorption cooling system designed with thermally evacuated tube collector and supported with a 60% LiBr–H_2O solution acts as absorption cooling system. The experiments were carried out in Nasiriyah city and thus delivering empirical data that can enhance the knowledge of its performance in Iraqi weather conditions. The most important conclusions are as follows;

1. Temperature of the generator is the basic factor affecting the operational of absorption cooling system, which depends on the intensity of the incident solar radiation.
2. The highest temperature that may be attained in August is 95 °C.
3. The best temperature of the evaporator was obtained as 28 °C on the 5th of August 2024.
4. The absorption cooling system operates in a sustainable efficient manner as it uses refrigerant that does not damage the Ozone layer, uses renewable energy to lessen the depletion of energy sources, and uses clean energy, which produces no waste gas that contributes to or worsens global warming.

Although the given research offers a useful amount of empirical evidence of what a solar-powered absorption cooling system was able to achieve in the context of the extreme summer settings of Nasiriyah, Iraq, the study is confined to the one-month-long experiment (August 2024) and the specific system design and capacity (1 kW). Further studies must thus revolve on seasonal appraisal over the long term to determine the variation of performance over the season, explore the effect of varying system scale and components optimization and carry out a thorough economic and environmental assessment to determine the viability of the large scale application in hot climate areas.

In conclusion, several useful observations can be derived from the present experimental results that can be useful for recent progresses in solar cooling [17–21]. Optimal generator (94 °C) and evaporator (28 °C) temperatures offer realistic operational limits for model validation and optimization of implementing PCM [17,18]. The tested experimental approach provides a repeatable framework for comparative energy-exergy analyses [19] and hybrid system designs [20] and the achieved performance with 945 W/m² solar radiation can inform material selection and sizing strategies for stand-alone adsorption applications [21]. The data presented in this paper and the fabrication technique discussed are useful for accelerating technologies and the use of next generation solar cooling technologies in hot climate regions.

Nomenclature

Symbol	Definition
a_1	First slope coefficient (W/m² °C)
a_2	Second slope coefficient (W/m² °C²)
COP	Coefficient of performance
I_T	Total incident solar radiation on the collector (W/m²)
T_a	Ambient temperature (°C)
ΔT	Temperature difference between ambient and collector outlet (°C)
η_c	Solar collector thermal efficiency
η_0	Zero-loss efficiency (optical efficiency)

References

[1] Allouhi, A., El Fouih, Y., Kousksou, T., Jamil, A., Zeraouli, Y., & Mourad, Y. (2015). Energy consumption and efficiency in buildings: current status and future trends. Journal of Cleaner production, 109, 118-130. https://doi.org/10.1016/j.jclepro.2015.05.139

[2] Mohammad, M. R., Mohammad, A. T., Al-Obaidi, M. A., Al-Shohani, W. A., & Albdeiri, M. S. (2025, June). Promoting Sustainability in Domestic Hot Water Sector: Analysis of Performance Indicators of an Evacuated Tube Solar Collector System. In IOP Conference Series: Earth and Environmental Science (Vol. 1507, No. 1, p. 012040). IOP Publishing. https://doi.org/10.1088/1755-1315/1507/1/012040

[3] Rashid, F. L., Al-Obaidi, M. A., Hussein, A. K., Akkurt, N., Ali, B., & Younis, O. (2022). Floating solar stills and floating solar-driven membranes: Recent advances and overview of designs, performance and modern combinations. Solar Energy, 247, 355-372. https://doi.org/10.1016/j.solener.2022.10.044

[4] Al-Obaidi, M. A., Rashid, F. L., Kadhim, S. A., Bouabidi, A., Alshammari, A., & Tolephih, M. H. (2025). Conical solar still with internal and external modifications: A comprehensive review. Green Technologies and Sustainability, 100324. https://doi.org/10.1016/j.grets.2025.100324

[5] Dahl, R. (2013). Cooling concepts: Alternatives to air conditioning for a warm world. Environmental Health Perspectives, 121(1), a18.https://doi.org/10.1289/ehp.121-a18

[6] Petela, K., & Szlęk, A. (2016). Assesment of Passive Cooling in Residential Application under Moderate Climate Conditions. Ecological Chemistry and Engineering. A, 23(2), 211-225. https://doi.org/10.1016/j.rser.2016.06.077

[7] Baniyounes, A. M., Rasul, M. G., & Khan, M. M. K. (2013). Assessment of solar assisted air conditioning in Central Queensland's subtropical climate, Australia. Renewable energy, 50, 334-341. https://doi.org/10.1016/j.renene.2012.06.042

[8] Balghouthi, M., Chahbani, M. H., & Guizani, A. (2008). Feasibility of solar absorption air conditioning in Tunisia. Building and environment, 43(9), 1459-1470. https://doi.org/10.1016/j.buildenv.2007.08.003

[9] Ketjoy, N., & Mansiri, K. (2013). Performance evaluation of 35 kW LiBr–H2O solar absorption cooling system in Thailand. Energy procedia, 34, 198-210. https://doi.org/10.1016/j.egypro.2013.06.748

[10] Martínez, P. J., Martínez, J. C., & Lucas, M. (2012). Design and test results of a low-capacity solar cooling system in Alicante (Spain). Solar Energy, 86(10), 2950-2960. https://doi.org/10.1016/j.solener.2012.06.030

[11] Burckhart, H. J., Audinet, F., Gabassi, M. L., & Martel, C. (2014). Application of a novel, vacuum-insulated solar collector for heating and cooling. Energy Procedia, 48, 790-795. https://doi.org/10.1016/j.egypro.2014.02.091

[12] Martínez, P. J., Martínez, J. C., & Lucas, M. (2012). Design and test results of a low-capacity solar cooling system in Alicante (Spain). Solar Energy, 86(10), 2950-2960. https://doi.org/10.1016/j.solener.2012.06.030

[13] Peuser, F. A., Remmers, K. H., & Schnauss, M. (2013). Solar thermal systems: Successful planning and construction. Routledge. https://doi.org/10.4324/9781315067247

[14] Balghouthi, M., Chahbani, M. H., & Guizani, A. (2005). Solar powered air conditioning as a solution to reduce environmental pollution in Tunisia. Desalination, 185(1-3), 105-110. https://doi.org/10.1016/j.desal.2005.03.073

[15] Hashemian, N., & Noorpoor, A. (2023). Thermo-eco-environmental investigation of a newly developed solar/wind powered multi-generation plant with hydrogen and ammonia production options. Journal of Solar Energy Research, 8(4), 1728-1737. https://doi.org/10.22059/jser.2024.374028.1388

[16] Hashemian, N., & Noorpoor, A. (2019). Assessment and multi-criteria optimization of a solar and biomass-based multi-generation system: Thermodynamic, exergoeconomic and exergoenvironmental aspects. Energy conversion and management, 195, 788-797. https://doi.org/10.1016/j.enconman.2019.05.039

[17] Al-Widyan, M.I, Amer, K.A., Ismail, M., Al-Assaf, A.H., & Abedalmuhdi Almomany, A. (2026). Solar-driven double-effect absorption cooling system with latent heat storage under Jordanian climatic conditions, Journal of Engineering Research. https://doi.org/10.1016/j.jer.2026.03.014

[18] Haile, D.M., & Alemu, D. (2026). Numerical model of solar-driven vapour absorption refrigeration integrated with phase change materials for sustainable sub-zero cooling. Journal of Engineering Research, 14(2), 2022-2042. https://doi.org/10.1016/j.jer.2025.12.008

[19] Kumi, E.N., Adunu, B.O., Owusu, J.S. (2026). Comparative energy-exergy evaluation of solar-assisted NH3-H_2 O and H2O-LiBr cooling systems under tropical conditions. Thermal Advances, 7,

100160
https://doi.org/10.1016/j.thradv.2026.100160.
[20] Wang, Q., Duan, L., Yang, Ch., Zhao, H., Liu, L., Zhang, H., Zheng, N., & Ding, X. (2026) Comprehensive sustainability assessment and energy analysis of a combined cooling, heating and power system integrated with high-temperature solar thermochemical complementation and low-temperature solar thermal collection processes. Renewable Energy, 261, 125212. https://doi.org/10.1016/j.renene.2026.125212
[21] Patel, J., Nakum, G., Mehta, P., Said, Z. (2026). Solar adsorption cooling systems for off-grid sustainability: Recent advances, design strategies, and future perspectives. Results in Engineering, 29, 108718.
https://doi.org/10.1016/j.rineng.2025.108718